NASA TECHNICAL NOTE

NASA TN D-5995

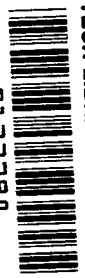

TESTS OF EVALUATED BERYLLIUM (n,2n) CROSS SECTIONS BY ANALYSIS OF 1.4-eV FLUX IN WATER FOR AN AMERICIUM-BERYLLIUM SOURCE ENCLOSED IN BERYLLIUM SPHERES

by Daniel Fieno, Roger L. Alexander, and C. Hubbard Ford

Lewis Research Center
Cleveland, Ohio 44135

NATIONAL AERONAUTICS AND SPACE ADMINISTRATION • WASHINGTON, D. C. • SEPTEMBER 1970

1. Report No. NASA TN D-5995	2. Government Accession No.	3. Recipient's Catalog No.
4. Title and Subtitle TESTS OF EVALUATED BERYLLIUM (n, 2n) CROSS SECTIONS BY ANALYSIS OF 1.4-eV FLUX IN WATER FOR AN AMERICIUM-BERYLLIUM SOURCE ENCLOSED IN BERYLLIUM SPHERES		5. Report Date September 1970
		6. Performing Organization Code
7. Author(s) Daniel Fieno, Roger L. Alexander, and C. Hubbard Ford		8. Performing Organization Report No. E-5444
9. Performing Organization Name and Address Lewis Research Center National Aeronautics and Space Administration Cleveland, Ohio 44135		10. Work Unit No. 129-02
		11. Contract or Grant No.
12. Sponsoring Agency Name and Address National Aeronautics and Space Administration Washington, D. C. 20546		13. Type of Report and Period Covered Technical Note
		14. Sponsoring Agency Code

15. Supplementary Notes

16. Abstract

Measurements in water of the neutron flux distributions at indium resonance energy, with Be shells enclosing an Am-Be neutron source, were made to quantitatively test two evaluated sets of (n, 2n) cross sections for ^{9}Be. Transport theory calculations of the experimental flux distributions have been made using cross sections from these two evaluations of the decay modes of the ^{9}Be(n, 2n) reaction. The first evaluation is based on the cross section program GAM-II in which the data files are based on the same cross section evaluation employed for the current ENDF/B library for Be. The second evaluation is based on Perkins' detailed studies of the reactions which contribute to the Be(n, 2n) cross section. Calculations using GAM-II data were in poor agreement with the present experiments whereas calculations using Perkins' data were in good agreement.

17. Key Words *(Suggested by Author(s))* Beryllium (n, 2n) reaction Neutron (α, n) sources	18. Distribution Statement Unclassified - unlimited

19. Security Classif. (of this report)	20. Security Classif. (of this page)	21. No. of Pages	22. Price*
Unclassified	Unclassified	39	$3.00

*For sale by the Clearinghouse for Federal Scientific and Technical Information Springfield, Virginia 22151

CONTENTS

	Page
SUMMARY	1
INTRODUCTION	2
DESCRIPTION OF EXPERIMENTS AND REDUCTION OF DATA	3
Source	3
Tank	3
Beryllium Spheres	3
Foils and Holder	4
Counters	4
Data Reduction	5
Counting Statistics	7
CALCULATIONAL METHODS AND CROSS SECTIONS	7
EXTIMATION OF A VIRGIN SPECTRUM	10
Review of Small Source Spectra	10
Derivation of a Consistent Virgin Source Spectrum	12
Source in air	13
Source in water	13
Accuracy of Calculational Procedure	17
COMPARISON OF CALCULATED RESULTS USING TWO EVALUATED Be(n, 2n) DATA SETS WITH MEASUREMENTS IN WATER FOR SOURCE ENCLOSED WITHIN BERYLLIUM SPHERES	18
Detailed Shapes of the Indium Resonance Energy Flux Distributions	18
Enhancement Due to Beryllium	20
CONCLUSIONS	23
REFERENCES	24

TESTS OF EVALUATED BERYLLIUM (n,2n) CROSS SECTIONS BY ANALYSIS OF 1.4-eV FLUX IN WATER FOR AN AMERICIUM-BERYLLIUM SOURCE ENCLOSED IN BERYLLIUM SPHERES

by Daniel Fieno, Roger L. Alexander, and C. Hubbard Ford
Lewis Research Center

SUMMARY

Measurements in water of the neutron flux distributions at indium resonance energy (1.4 eV), with beryllium (Be) shells enclosing an americium-beryllium (Am-Be) neutron source, were made to quantitatively test two evaluated sets of (n,2n) cross sections for ^{9}Be. Multigroup Sn calculations of the experimental flux distributions have been made using cross sections from these two evaluations of the decay modes of the ^{9}Be(n,2n) reaction. The first evaluation is based on the data files of the GAM-II program which use the same cross section evaluation employed for the current ENDF/B library for Be. The second evaluation is based on Perkins' detailed studies of the reactions which contribute to the ^{9}Be(n,2n) cross section.

This work required an accurate evaluation of the spectrum of the neutron source. An uncollided source spectrum was obtained which, when used in an S_n calculation, gave agreement with the measured flux distribution for the source in water. The neutron leakage spectrum computed for the source in air using this uncollided spectrum was also required to match a measured leakage spectrum.

Tests of the evaluated ^{9}Be(n,2n) cross sections are made by analysis of measurements in water of the flux distributions for the Am-Be source enclosed in Be spheres. The calculations using cross sections for Perkins' Be(n,2n) evaluation gave good agreement with the experiments. Calculations with Be(n,2n) cross sections obtained from the data files of the GAM-II code gave poor agreement with these experiments.

For the Am-Be source in the 1.9-centimeter-thick Be shell, the computed enhancements at 1.4-eV are 9.4 and 9.5 percent for calculations using Perkins' Be(n,2n) data and GAM-II Be data, respectively. The experimental enhancement is measured to be 7.3±2.0 percent. For the Am-Be source in the 7.0-centimeter-thick Be shell, the computed enhancements are 26.3 and 27.6 percent for calculations using Perkins' Be(n,2n) data and GAM-II Be data, respectively. The experimental enhancement is measured to be 22.8±2.5 percent.

The calculation of the shape of the spatial distribution of 1.4-eV energy neutrons and values of enhancement using Perkins' Be(n,2n) data are significantly better than using the GAM-II Be(n,2n) data. Since current ENDF/B cross sections are based on the same evaluation as used to formulate the GAM-II cross sections, it is suggested that Perkins' evaluation be used to update cross sections for Be.

INTRODUCTION

Analysis of reactors using beryllium (Be) or beryllium oxide as either a moderator or a reflector requires accurate calculation of the so-called fast multiplication effect due to (n, 2n) reactions. Precise criticality calculations have been hampered by an incomplete knowledge of the decay modes of the Be(n, 2n) reaction and large discrepancies in both the fast effect and age still exist (ref. 1). Since beryllium is of considerable importance to nuclear reactors, it is essential to assess by means of additional experiments the relative applicability of various models for the Be(n, 2n) reaction.

In the present experiments measurements of the neutron flux distribution at indium resonance energy were made in water for an americium-beryllium (Am-Be) neutron source enclosed by beryllium shells. Multigroup transport theory calculations of these experimental flux distributions are compared using two evaluations of the Be(n, 2n) cross sections. Thus, the calculated as compared to the measured flux distributions provide quantitative indications of the relative effects of various cross section evaluations of the decay modes of the Be(n, 2n) reaction.

Two Be(n, 2n) cross section evaluations are considered for this study. The first evaluation is based on a widely used cross section program, GAM-II (ref. 2), which grossly approximates the Be(n, 2n) reaction mechanism in computing the multigroup neutron transfer cross sections. The GAM-II cross sections are based on an evaluation of Joanou and Stevens (ref. 3) which also serves as a basis for the present ENDF/B cross section library for Be (ref. 4). The second evaluation is based on the work by Perkins described in references 5 to 7 which presents detailed evaluations of the Be(n, 2n) cross sections and provides calculations of the angular and energy distributions for neutrons from the various decay modes of the ^{9}Be(n, 2n) reaction. This work by Perkins provides a more comprehensive evaluation of the multigroup transfer cross sections for beryllium.

In the first part of the present study an uncollided or virgin spectrum was constructed for the Am-Be source by means of S_n transport calculations for two experiments. In the first experiment a leakage or collided spectrum for the source in air was measured using an NE-213 proton recoil scintillator. In the second experiment the indium resonance energy flux distribution was measured for the source in an effectively infinite water medium. By an iterative procedure, a virgin spectrum was obtained which correctly calculated this flux distribution in water, as well as reproduced the measured source leakage spectrum in air. This virgin spectrum was required not to exceed the estimated limits of error of published small source spectra measured by several independent techniques.

The second part of this work employs the Am-Be source, enclosed by spherical shells of Be, in an infinite medium of water to measure the neutron flux distributions

at indium resonance energy. Multigroup S_n transport calculations are compared to corresponding experimental flux distributions and to source enhancements due to Be.

DESCRIPTION OF EXPERIMENTS AND REDUCTION OF DATA

Flux distributions at indium resonance energy were measured in water for three different spherical configurations: for the Am-Be source alone and for the source at the center of each of two beryllium spheres.

Source

The spherical Am-Be neutron source contains 54 curies (2×10^{12} disintegrations/sec) of ^{241}Am (16.7 g) in a net volume of 84.3 cubic centimeters. There are 4.0±0.4 grams of beryllium for each gram of ^{241}Am, thus giving a total of 66.8±6.7 grams of Be in the source. The output of the source was $(1.30\pm0.08)\times10^{8}$ neutrons per second in January 1967.

The outer surface of the source is spherical (6.096-cm outside diameter) and includes two stainless steel containment shells, one 0.140 centimeter thick and the other 0.152 centimeter thick. The dimension of the spherical cavity for the source material is 5.462 centimeters inside diameter. The Am-Be material was pressed in the inner two hemispheres and a spring was placed between the two before welding.

Tank

For all experiments except the bare source in water, the indium resonance energy flux distributions were measured in a cylindrical tank of demineralized water that was 2.44 meters outside diameter by 2.44 meters high. The tank used for the bare source in water experiment was 1.83 meters outside diameter by 1.52 meters high. Both tanks provided an effectively infinite water medium for these configurations.

Beryllium Spheres

The two spheres used were the following:

(1) 10.16-centimeter outside diameter Be sphere (1.9-cm shell thickness)

(2) 20.32-centimeter outside diameter Be sphere (7.0-cm shell thickness)

All spheres were made of hemispheres. The beryllium hemispheres were made with a

6.35-centimeter inside diameter central space to accommodate the source. To center the source and also displace any water, an aluminum spherical shell 0.127 centimeter thick was placed around the source.

Foils and Holder

To measure the neutron flux distributions at indium (In) resonance energy, indium foils 4.99 centimeters outside diameter by 0.0127 centimeter thick were used. The large diameter foils were required so that measurements could be made as far as 80 centimeters from the bare source in water. These foils were covered all around by cadmium 0.089 centimeter thick corresponding to a cutoff energy of 0.6 eV. The activity of the irradiated foils is then proportional to the 54-minute half-life ^{116}In activity. The 4.4-hour half-life ^{115}In activity caused by inelastic scattering of neutrons above about 1 MeV was small because the high energy flux decreases rapidly as a function of distance in water and because irradiations close to the source were of short duration of the order of 30 minutes. Measurements as far as approximately 100 centimeters from the source were made with these foils in aluminum covers.

A lucite holder was used to position the foils. Figure 1 shows the foil holder positioned over a sphere. The three legs were notched to locate the cadmium covered foils. The notches were spaced every 1.27 centimeters for the first 11.43 centimeters and every 2.54 centimeters from there on out to nearly 150 centimeters. No two foils were ever placed closer than 7.62 centimeters apart during any one irradiation.

Counters

Each foil was counted on both sides in several 2π beta counters. Counter plateaus were obtained periodically using irradiated indium foils and carbon 14 (^{14}C). The use of several counters provided a check of counter stabilities during the counting periods. Counter efficiencies were not measured. To reduce background counts, one of the hemispherical counters of radius 2.86 centimeters was equipped with an anticoincidence scintillation region which surrounded all but the bottom of the counter. A minimum-ionizing muon will dissipate at least 3 MeV in this scintillator. An approximately 1-MeV threshold was obtained by setting the scintillator voltage at the point where cobalt 60 (^{60}Co) gammas began to be detected. Thus, most background counts caused by muons are subtracted. This particular counter background was reduced to about 1.7 counts per minute from about 23 counts per minute. Foil backgrounds were counted in each counter prior to each irradiation. This background measurement becomes important for those foils located in the water far from the source.

Data Reduction

Counting data were reduced using the following equation:

$$C_{s,m} = \frac{C + L - B}{\left(e^{-t_w/\tau}\right)\left[\tau\left(1 - e^{-t_c/\tau}\right)\right]\left(1 - e^{-t_i/\tau}\right)} \tag{1}$$

where

B	foil background
C	raw counts
L	dead time counting loss, $(t_d/t_c)C^2$
t_c	count time, min
t_d	dead time, min
t_i	irradiation time, min
t_w	time from end of irradiation to start of count, min
τ	half-life/ln 2 (mean life, min)

$C_{s,m}$ is the measured saturated foil count rate as opposed to a saturated activity since counter efficiencies were not measured. The average $C_{s,m}$ computed for the foil front sides was averaged with the average $C_{s,m}$ for the foil back sides. This average $\overline{C}_{s,m}$ is taken to be proportional to the indium resonance energy flux (ref. 8).

Foil size corrections were made to account for the geometric variation of fluxes over the various segments of each foil. Different portions of these large foils were at different distances from the center of symmetry. The data were corrected using the following equation (ref. 9):

$$C_s(r_0) = \overline{C}_{s,m}(r_0) - \frac{r_f^2}{4r_0}\left[\frac{d\overline{C}_{s,m}(r_0)}{dr}\right] \tag{2}$$

where

$\overline{C}_{s,m}(r_0)$	measured saturated foil count rate at r_0
$d\overline{C}_{s,m}(r_0)/dr$	approximation to flux derivative at r_0
r_f	foil radius, cm
r_0	distance from source center to center of foil, cm

TABLE I. - EXPERIMENTAL INDIUM RESONANCE ENERGY ACTIVITY FOR Am-Be NEUTRON SOURCE IN INFINITE WATER MEDIA

[Data normalized using equation (4b).]

Source alone			10.16-cm o.d. Be sphere around source[a]			20.32-cm o.d. Be sphere around source[a]		
Radius, cm	Corrected counts, C_s	Error	Radius, cm	Corrected counts, C_s	Error	Radius, cm	Corrected counts, C_s	Error
3.46	0.1470E-03	0.59E-06	5.50	0.1287E-03	0.23E-06	10.57	0.9801E-04	0.52E-06
4.73	.1377E-03	.11E-06	6.67	.1150E-03	.50E-06	11.84	.7813E-04	.38E-06
6.00	.1152E-03	.10E-06	8.04	.9449E-04	.16E-05	13.11	.5651E-04	.28E-06
7.27	.9015E-04	.92E-07	9.31	.7215E-04	.79E-06	14.38	.3877E-04	.24E-06
8.54	.6730E-04	.52E-07	10.57	.5154E-04	.22E-06	15.65	.2585E-04	.37E-06
9.81	.4982E-04	.62E-07	11.87	.3674E-04	.45E-06	16.92	.1730E-04	.17E-06
11.08	.3561E-04	.39E-07	13.12	.2672E-04	.16E-06	18.19	.1169E-04	.38E-07
12.35	.2670E-04	.36E-07	14.39	.1907E-04	.67E-07	19.46	.8212E-05	.46E-07
14.89	.1463E-04	.45E-07	15.66	.1411E-04	.12E-06	20.73	.5797E-05	.45E-07
17.43	.8336E-05	.18E-07	16.94	.1033E-04	.57E-07	22.00	.4182E-05	.26E-07
19.97	.5046E-05	.17E-07	19.48	.5747E-05	.10E-06	24.54	.2349E-05	.20E-07
22.51	.3101E-05	.10E-07	22.00	.3529E-05	.41E-07	27.08	.1383E-05	.16E-07
25.05	.1895E-05	.28E-07	27.09	.1299E-05	.35E-07	29.62	.8451E-06	.56E-08
30.13	.7755E-06	.38E-08	32.17	.5259E-06	.76E-08	32.16	.5331E-06	.15E-07
32.67	.5052E-06	.26E-08	37.25	.2352E-06	.49E-08	34.70	.3401E-06	.25E-08
35.21	.3446E-06	.27E-08	39.79	.1540E-06	.31E-08	37.24	.2236E-06	.33E-08
37.75	.2314E-06	.34E-08	44.87	.7517E-07	.60E-08	39.78	.1476E-06	.38E-08
40.29	.1507E-06	.55E-08	49.95	.3541E-07	.15E-08	42.32	.9876E-07	.94E-09
42.83	.1013E-06	.17E-08	52.49	.2247E-07	.17E-08	44.86	.6606E-07	.10E-08
45.37	.6685E-07	.11E-08	57.57	.1165E-07	.96E-09	47.40	.4601E-07	.11E-08
47.82	.5086E-07	.11E-08	65.19	.3732E-08	.28E-09	49.94	.3068E-07	.16E-08
50.45	.3322E-07	.12E-08	67.73	.2672E-08	.73E-10	52.48	.2151E-07	.72E-09
52.99	.2301E-07	.64E-09	70.27	.1826E-08	.37E-09	55.02	.1477E-07	.29E-09
55.53	.1619E-07	.48E-09	72.81	.9449E-09	.26E-09	57.56	.1039E-07	.37E-09
58.07	.1096E-07	.42E-09				60.10	.7258E-08	.39E-09
60.61	.7731E-08	.27E-09				62.64	.4477E-08	.76E-09
63.15	.6108E-08	.83E-09				65.18	.3475E-08	.45E-09
65.69	.4349E-08	.37E-09				67.72	.2538E-08	.44E-09
68.23	.3273E-08	.21E-09				70.26	.1458E-08	.24E-09
70.76	.2203E-08	.32E-09						
73.27	.1291E-08	.35E-09						
75.84	.9255E-09	.23E-09						
80.92	.5192E-09	.24E-09						

[a]Source is centered in Be spheres by 0.127-cm-thick aluminum spherical shell.

Counting Statistics

Counting statistics were calculated in several ways. Theoretical errors, that is, the square root of the number of counts, were obtained for each count. Also for each counter a standard deviation of the saturated count rate was calculated. Composite errors were calculated over all counters for both the theoretical and standard errors. These composite errors were then compared to a standard deviation of all the $C_{s,m}$'s for a particular foil as though the results from all counters were part of the same distribution. Counter plateau shifts or noise problems could be seen easily in this way. Composite errors were obtained in all cases with the $C_{s,m}$ from front and back sides of the foil combined to give an average value $\overline{C}_{s,m}$.

Finally, when measurements at a given radius were repeated, the standard deviation of the $\overline{C}_{s,m}$ and a composite error were again computed. The larger error is reported here. The distribution data and the errors are listed in table I for the three experiments with the Am-Be neutron source.

CALCULATIONAL METHODS AND CROSS SECTIONS

Multigroup calculations using the S_n formulation of transport theory were used to obtain the indium resonance energy flux distributions for all of the experiments considered. The formulation of this method is given in an appendix of reference 10. The calculations were all done in spherical geometry with an effectively infinite water region, the outer boundary radius being greater than 110 centimeters. The Am-Be neutron source and its stainless steel container were explicitly included in the calculations both as to dimensions and composition. The calculations were for a fixed source using a virgin spectrum and a uniform distribution throughout the source region.

Thirty energy groups were used to describe the spectrum for the various configurations considered. The details of this group structure are presented in table II. For convenience, group 28 which extends in energy from 1.125 to 1.445 eV, was chosen as the group representative of the indium resonance activation energy.

Two computer programs were used to provide the group averaged microscopic cross sections for all of the isotopes used in the calculations. These programs are GAM-II (ref. 2) and GATHER-II (ref. 11). The GAM-II program also provided one of the evaluations for the P_0 down scattering transfer cross sections for the Be(n, 2n) reaction.

GAM-II is a B_3 multigroup code for the calculation of fast neutron spectra. For this study, the code was used to integrate the B_3 equations over 99 energy groups covering the energy range from 14.92 MeV to 0.414 eV. The cross sections for the

TABLE II. - 30-GROUP ENERGY AND

LETHARGY BOUNDARIES

Group	Upper energy boundary, eV[a]	Lethargy boundary	Lethargy width
1	1.105×10^{7}	-0.1	0.1
2	1.000×10^{7}	0	↓
3	9.048×10^{6}	.1	
4	8.187×10^{6}	.2	
5	7.408×10^{6}	.3	
6	6.703×10^{6}	.4	
7	6.065×10^{6}	.5	
8	5.488×10^{6}	.6	
9	4.966×10^{6}	.7	
10	4.493×10^{6}	.8	↓
11	4.066×10^{6}	.9	.2
12	3.329×10^{6}	1.1	.2
13	2.725×10^{6}	1.3	.3
14	2.019×10^{6}	1.6	.4
15	1.353×10^{6}	2.0	.5
16	8.209×10^{5}	2.5	.7
17	4.076×10^{5}	3.2	.7
18	2.024×10^{5}	3.9	.85
19	8.652×10^{4}	4.75	1.50
20	1.931×10^{4}	6.25	1.75
21	3.355×10^{3}	8.0	1.25
22	961.1	9.25	1.0
23	353.6	10.25	↓
24	130.1	11.25	
25	47.85	12.25	↓
26	17.60	13.25	1.25
27	5.043	14.50	1.25
28	1.445	15.75	.25
29	1.125	16.0	1.0
30	.414	17.0	----

[a]Thermal group (group 30) lower energy boundary is 0.001 eV.

29 fast groups are obtained by averaging over the 99-group spectrum obtained for a given material composition. Down scattering transfer cross sections for elastic scattering through the P_3 order are included for all isotopes.

GATHER-II was used to obtain thermal, or 30^{th} group, cross sections. This program is a P_1 code for the calculation of thermal spectra over 101 energy points covering the energy range from 2.38 to 0.001 eV. All of the cross sections obtained using the GATHER-II program are based on a temperature of 293 K.

The P_0 down scattering transfer matrix for the Be(n, 2n) reaction in the GAM-II data files is based on the evaluation of Joanou and Stevens (ref. 3). This evaluation gives a total cross section for the Be(n, 2n) reaction as well as partial cross sections for the excitation of the 2.43- and 1.75-MeV levels. These cross sections are shown in figure 2(a) for comparison with the evaluated Be(n, 2n) cross section data of Perkins (ref. 5) which is shown in figure 2(b). Both evaluations of the total Be(n, 2n) cross sections are in agreement. However, the GAM-II evaluation of the decay modes of the Be(n, 2n) reaction are in disagreement with the evaluation due to Perkins.

The largest contribution to the Be(n, 2n) reaction in Perkins' evaluation comes from the excitation of the 2.43-MeV level in $^{9}Be^{*}$. The majority (91.7 percent) of these reactions are assigned as leaving $^{8}Be^{*}$ in a broad 2.90-MeV excited state with an effective excitation energy in ^{8}Be of 0.6 MeV. The remaining reactions go to the ground state of ^{8}Be. Smaller cross sections for the excitation of levels in $^{9}Be^{*}$ at 6.76 and 9.1 MeV are also assigned by Perkins.

The remaining cross section which is a large fraction of the Be(n, 2n) cross section at lower energies proceeds by multibody breakup. Two multibody models for energy and momentum transfer are ordinarily considered. One is the cluster model. In this model, after inelastic scattering of a neutron with ^{9}Be, the residual $^{8}Be^{*}$ nucleus and the second neutron move together, finally separating. This model is indistinguishable from the excited state reaction in which the $^{9}Be^{*}$ nucleus is left in the 1.70-MeV excited state. In this case, the excitation energy of the $^{8}Be^{*}$ nucleus shared with the second neutron is small (35 keV). The second model partitions the energy in proportion to the momentum phase volume. The reactions of interest are the three-body breakup $^{9}Be(n, 2n)^{8}Be^{*}$ and the four-body breakup $^{9}Be(n, 2n)2\alpha$. This report assumes that the multibody breakup to the ^{8}Be ground state proceeds by the three-body phase space model rather than the cluster model.

The evaluation of the reported Be(n, 2n) data by Perkins (ref. 5) was used to compute the Be(n, 2n) P_0 down scattering transfer matrix using the AGN-SIGMA code (ref. 7). In the present report, this evaluation of the Be(n, 2n) data is referred to simply as Perkins' Be data. The P_0 down scattering cross sections based on GAM-II are radically different from Perkins' Be data. Figure 3 shows a comparison of the P_0 down scattering data for several neutron energies using the GAM-II evaluation and Perkins' evaluation. For an incident neutron energy of 9.5 MeV the GAM-II P_0 down scattering data as shown in figure 3(a) extends down to 3.7 MeV while Perkins' Be data extends below 0.1 MeV. Similar results obtained for incident neutron energies of 5.8 and 3.5 MeV are shown in figures 3(b) and (c).

For the transport calculations the number of energy groups, the elastic scattering order, and the type and order of the quadrature set used in the S_n calculations are important. Mynatt, Greene, and Engle (ref. 12) found that elastic scattering treated to

TABLE III. - GAUSS-LEGENDRE QUADRATURE SET FOR S_{16} TRANSPORT CALCULATIONS IN SPHERICAL GEOMETRY

Direction number	Direction cosine	Weight
1	-1.0	0
2	-.9894009	.0135762
3	-.9445750	.0311268
4	-.8656312	.0475793
5	-.7554044	.0623145
6	-.6178762	.0747980
7	-.4580168	.0845783
8	-.2816036	.0913017
9	-.0950125	.0947253
10	.0950125	.0947253
11	.2816036	.0913017
12	.4580168	.0845783
13	.6178762	.0747980
14	.7554044	.0623145
15	.8656312	.0475793
16	.9445750	.0311268
17	.9894009	.0135762

P_3 order with an S_{16} quadrature was adequate for obtaining the neutron dose rate in water. The results reported herein use an S_{16} Gauss-Legendre quadrature set (ref. 13) which has also been shown to be adequate for obtaining the fast neutron dose rate in a water medium. This quadrature set is listed in table III.

ESTIMATION OF A VIRGIN SOURCE SPECTRUM

Review of Small Source Spectra

A review article by Hanson (ref. 14) covers much of the work on (α, n) sources up to about 1958. The dominant reaction in beryllium for alpha energies up to about 6 MeV is (refs. 15 to 17):

$$^{9}Be + {}^{4}He \rightarrow {}^{12}C + n + 5.708 \text{ MeV}$$

The ^{12}C nucleus can be left in the ground state or in excited states at 4.43 or 7.65 MeV.

For polonium 210 (^{210}Po) alphas (E_α = 5.30 MeV), the maximum neutron energy is about 10.9 MeV.

Although measurement of the total ^{9}Be(α, n) cross section (refs. 15 to 17) is reasonably complete and the partial cross sections leading to the ground state and first excited state of ^{12}C have been measured (ref. 18), calculations of source spectra are not too satisfactory (ref. 19). Transitions to other than the ground and 4.43-MeV states of ^{12}C are accompanied by low energy neutrons so these partial cross sections are difficult to measure. St. Romain, Bonner, Bramblett, and Hanna (ref. 20) using Bonner spheres observed a group of neutrons at about 0.3 MeV for alpha particles with about 5-MeV energy. These neutrons were in addition to those from the 7.65-MeV level of ^{12}C which were not abundant (ref. 21). It was suggested (ref. 20) that low energy neutrons may be produced from endoergic breakup reactions in Be

$$^{4}\text{He} + {}^{9}\text{Be} \rightarrow {}^{4}\text{He} + \left[{}^{9}\text{Be}^{*} \rightarrow {}^{8}\text{Be} + \text{n} - 1.665\ \text{MeV}\right]$$

or

$$\left[{}^{9}\text{Be}^{*} \rightarrow 2({}^{4}\text{He}) + \text{n} - 1.564\ \text{MeV}\right]$$

where the excited level in ^{9}Be is at 2.43 MeV or possibly at 1.70 MeV.

In this work, reported spectra of several small ^{210}Po-Be sources were studied to obtain what is thought to be a reasonable estimate of the virgin or uncollided neutron source spectrum. The virgin spectrum of neutrons from either plutonium 239-beryllium (^{239}Pu-Be) (E_α = 5.15 MeV) or ^{241}Am-Be (E_α = 5.48 MeV) should be very similar to ^{210}Po-Be (E_α = 5.30 MeV). However, the number of low energy neutrons from the endoergic fraction increases with alpha energy. So the fraction of low energy neutrons in a virgin source may be expected to be greatest in ^{241}Am-Be sources.

The spectra of neutrons from ^{210}Po-Be sources have been measured many times by a variety of methods. An early measurement is that of Whitmore and Baker (ref. 22) who used photographic emulsions. Notarrigo, Parisi, Ricamo, and Rubbino (ref. 23) used emulsions and reviewed the measurements up to 1961. They also made a calculation of the source spectrum on an isotropic (α, n) angular cross section hypothesis. Haag and Fuchs (ref. 24) in 1962 used a stilbene crystal spectrometer following the method of Broek and Anderson (ref. 25). One of the latest measurements, by Freestone, Muckenthaler, Straker, and Henry (ref. 26) at Oak Ridge (1967), used a similar technique but with the NE-213 liquid scintillator (ref. 27). They show essentially identical results for spectra of small ^{239}Pu-Be, ^{210}Po-Be, and ^{241}Am-Be sources.

Each method of measurement has sources of error. In the emulsion method, emulsion shrinkage upon development, loss of track length through the surface, and difficulty

in identifying and measuring extremely short low energy track lengths are typical problems. In a stilbene scintillator, anisotropy of light output with track orientation occurs. In an NE-213 scintillator, self-absorption of light and inability to distinguish between neutron and gamma induced events at small light output are problems. Both stilbene and NE-213 exhibit a strong nonlinearity of proton light response with energy. The shape of Haag and Fuchs' spectrum at low energy may reflect an overcompensation for this effect. None of the methods are satisfactory much below 1 MeV.

Figure 4 shows several measured Po-Be neutron spectra normalized to a yield of 0.88 neutron over the energy range from 1 to 11 MeV; a yield of 0.12 below 1 MeV will be shown to be necessary for the interpretation of the present source experiments. All show broad maxima from 3 to 5 MeV. Most of these neutrons come from reactions leaving ^{12}C in the 4.43-MeV excited state. Smaller maxima near 7 and 9.5 MeV arise out of anisotropy of the ground state branch (ref. 17). Freestone, Muckenthaler, Straker, and Henry (ref. 26) and Whitmore and Baker (ref. 22) are in best agreement, showing small differences. The spectrum of Haag and Fuchs is somewhat harder than the others.

Various authors have suggested the presence of a large contribution to the total source spectrum below 1 MeV. St. Romain, Bonner, Bramblett, and Hanna studied a Pu-Be source that contained 13 grams Pu and probably 7 grams Be. By use of the Bonner sphere response functions, they assigned about 16 percent of the neutrons below 1 MeV in this source, with a peak at 0.3 MeV. Contributions to this portion of the spectrum from scattering and (n, 2n) reactions in beryllium are estimated to reduce the fraction of low energy virgin neutrons in this source by about 3 percent of the total. Geiger and Hargrove (ref. 28) measured the spectrum of a small Am-Be source that contained 3 grams of Be alloyed with 0.23 grams of Am, enclosed in stainless steel 0.13 centimeter thick. They calculated 17 percent of the neutrons in their spectrum below 1.5 MeV. These data indicate that a virgin Po-Be spectrum contains a significant fraction below 1 MeV.

A preliminary virgin spectrum was obtained from the data of figure 4. The shape from 1 to 11 MeV was constructed from the spectra shown by weighting the Whitmore and Baker and Freestone spectra twice as much as the other two measured spectra. The fraction from 0 to 1 MeV followed the shape given by St. Romain from 0 to 0.6 MeV. This is shown in figure 4 as a dashed segment from 0 to 1 MeV. These yield shapes above and below 1 MeV were used to obtain a virgin spectrum that was compatible with the present experiments for the Am-Be source in air and in water.

Derivation of a Consistent Virgin Source Spectrum

An uncollided or virgin spectrum was constructed for the Am-Be source by means

of S_n transport calculations for two experiments using the preliminary virgin spectrum of the previous section as a starting point. In the first experiment a leakage or collided spectrum for the source in air was measured using an NE-213 proton recoil scintillator. In the second experiment the indium resonance energy flux distribution was measured for the source in an effectively infinite water medium. By an iterative procedure using the S_n method, a virgin spectrum was obtained which satisfied both experiments. This virgin spectrum was constrained not to exceed the estimated limits of error of published small source spectra measured by several independent techniques.

Source in air. - The leakage spectrum for the Am-Be source in air was measured using an NE-213 proton recoil scintillation spectrometer. In the experiment, the Am-Be source was mounted 370 centimeters above an earthen mound to minimize wall and ground scattering. The top of the mound is about 9 meters long by 6 meters across and about 6 meters above ground. The source was supported by a 0.64-centimeter-diameter brass rod positioned in an aluminum tube.

The measured Am-Be source leakage spectrum down to 0.5 MeV, obtained with an NE-213 proton recoil scintillation spectrometer and analyzed by the FERDOR computer program (ref. 29), is shown in figure 5. The solid histogram in figure 5 is the calculated leakage spectrum using the yield shapes above and below 1 MeV as shown in figure 4 and Perkins' evaluation for the (n, 2n) cross sections for the source beryllium. The required virgin spectrum is shown as the dashed line.

The agreement of the calculation with the measurement of the flux per unit energy and per source neutron at 2 meters from the Am-Be source in air is very good over the energy range from 2 to 8 MeV. For the small neutron yields from 8 to 11 MeV, the calculation is lower than the measured data. Below 2 MeV the calculation is in good agreement with the measured data. Thus, the virgin source spectrum listed in table IV along with Perkins' Be(n, 2n) data gives a calculated leakage spectrum using the S_n method which fits the measured data quite well.

Source in water. - Slowing down of neutrons in water is well understood. The spatial distribution of the indium resonance energy flux can provide additional evidence of the validity of the assigned source energy spectrum and the calculational method. Source neutrons of a given energy give a characteristic spatial distribution of the indium resonance energy flux. This can be seen from the distributions plotted in figure 6 for a number of point monoenergetic sources in water. The energy of the various monoenergetic sources corresponds to the average energy of a number of the energy groups listed in table II. The flux age for the various distributions are also listed in figure 6. The calculations were performed using P_3S_{16} multigroup transport theory and correspond to a source strength of 1 neutron per second.

Indium resonance energy flux distributions calculated for point monoenergetic sources having the average energy of each group listed in table II, result in an indium

TABLE IV. - FRACTIONAL ESTIMATED VIRGIN SOURCE AND GROUP AVERAGED Be(n, 2n) CROSS SECTIONS FOR 30-GROUP SPLIT OF TABLE II

Group	Total Be(n, 2n) cross section, b		Virgin source fraction
	GAM-II data	Perkins' data	
1	0.559	0.528	0.00862
2	.569	.583	.02222
3	.579	.594	.03534
4	.592	.596	.05469
5	.600	.596	.05650
6	.605	.600	.06156
7	.606	.597	.07081
8	.603	.597	.07632
9	.600	.593	.07572
10	.590	.582	.07390
11	.565	.533	.12078
12	.376	.296	.09703
13	.026	.039	.07858
14	.00001	.0007	.02786
15	0	0	.04087
16			.0469
17			.0433
18			.006
19			.003
20			0
21			
22			
23			
24			
25			
26			
27			
28			
29			
30			

resonance energy flux distribution in water $\varphi(r)$ for a distributed source spectrum given by

$$\varphi(r) = \sum_g f_g \varphi_g(r) \tag{3}$$

In equation (3) the quantity f_g is the source fraction in group g and $\varphi_g(r)$ is the indium resonance energy flux at distance r from a point source having the average energy of group g.

Although the spatial distributions shown in figure 6 can be used to obtain indium resonance energy flux distributions in water for a given source spectrum, direct multigroup S_n calculations are made that account for the source size and composition as well as the stainless steel container. An indium resonance energy flux distribution from a 30-group P_3S_{16} transport calculation using the virgin source spectrum listed in table IV is shown in figure 7. Figure 7 also shows the normalized count rates multiplied by the square of the radius $C_s r^2$ for the Am-Be source in water.

Both the measured and calculated indium resonance energy flux distributions shown in figure 7 are normalized such that the volume integral of the slowing down density is unity. The total number of neutrons Q slowing down past indium resonance energy is given by

$$Q = \int_0^\infty q(r)dV \tag{4a}$$

where the slowing down density q(r) equals the product of the slowing down power of the medium times the flux. The quantity dV is the element of volume. For the experiments the measured count rate C_s is taken as proportional to the flux so that equation (4a) may be rewritten as

$$Q' = n \int_0^\infty k(r) \begin{Bmatrix} C_s(r) \\ \text{or} \\ \varphi(r) \end{Bmatrix} dV \tag{4b}$$

where k(r) is the ratio of the slowing down power of the medium at r to that of water.

In table I are given the normalized experimental saturated front and back averaged count rates of the indium foils C_s measured for the Am-Be source in water. These data have also been corrected for foil size effect according to equation (2). The normalization factor $n = 1.837 \times 10^{-10}$ is the factor required to make $Q' = 1$ in the experiment with the source in water. This same normalization factor is used in the treatment of the other experiments in water with beryllium shells around the source. As indicated, the calculations are normalized in a similar manner.

The logarithm of the normalized count rates $C_s r^2$ data shown in figure 7 can be fitted by a straight line within the experimental error at distances greater than 25 centimeters. If thermal neutron activation data for indium, not listed in table I, are normal-

ized between 45 and 65 centimeters to the indium resonance energy activity, the straight line fit extends out to 100 centimeters from the source. The measured data are thus fitted by the approximation

$$C_s r^2 = A \exp\left(-\frac{r}{\lambda}\right) \tag{5}$$

By using a least squares technique, the characteristic relaxation length λ obtained is 9.54±0.10 centimeters. This least squares fit to the measured data beyond 25 centimeters obtained from equation (5) is shown as the dashed line in figure 7.

In figure 7 the solid line shows the flux distribution from the 30-group P_3S_{16} transport calculation. The virgin source spectrum used was obtained by first using a virgin spectrum consistent with the leakage spectrum for the source in air and then modifying it to obtain agreement with the experiment by means of the P_3S_{16} calculation of the flux distribution in water. As mentioned before, the source fraction in each group was subject to the constraint of being within the estimated bounds of the published small-source measurements. The virgin source fraction required below 1 MeV for best fit was almost exactly 12 percent, similar to the original estimate for the source in air.

Calculated and measured parameters such as the flux age and higher spatial moments can be compared for a finite sized source. The m^{th} even spatial moment $\overline{r^m}$ for the indium resonance energy flux distribution $\varphi(r)$ in an infinite spherical medium is defined as

$$\overline{r^m} = \frac{\int_0^\infty r^m \varphi(r) dV}{\int_0^\infty \varphi(r) dV} \qquad (m = 0,\ 2,\ 4,\ 6,\ \ldots) \tag{6}$$

The flux age τ is one-sixth of the mean square of the distance $\overline{r^2}$ from the source at which neutrons possess indium resonance energy. In table V are some of the calculated and measured parameters for the source in water. These parameters also indicate the closeness of the fit established for the source in water with calculations based on the virgin source spectra. For example, the calculated flux age τ is 55.5 square centimeters as compared to the measured 56.0±1.2 square centimeters for the finite sized Am-Be source in water.

Calculated neutron flux spectra at a number of radii of figure 7 are shown in figure 8 for the source in water. The mean energy of the flux spectrum at each radius is shown by the symbol on the curve. The mean energy and flux spectrum change only slowly with radius past about 10 centimeters.

TABLE V. - PARAMETERS OF EXPERIMENTAL AND CALCULATED INDIUM RESONANCE ENERGY FLUX DISTRIBUTIONS FOR Am-Be SOURCE IN WATER

	Experimental	Calculated
Second moment, $\overline{r^2}\times10^{-2}$, cm^2	3.360 ([a]1.1)	3.331 ([b]3.363)
Fourth moment, $\overline{r^4}\times10^{-5}$, cm^4	3.92 ([a]7.6)	3.93 ([b]4.02)
Sixth moment, $\overline{r^6}\times10^{-8}$, cm^6	10.81 ([b]25.9)	11.23 ([b]11.63)
Relaxation length, λ, cm	9.54±0.10	----------
Flux age, τ, cm^2	56.0±1.2	55.5 ([b]56.1)

[a]Percent extrapolation for numerator (percent extrapolation for denominator ~0.1).

[b]P_3S_{32} calculation.

Accuracy of Calculational Procedure

A few remarks are in order concerning the validity of the comparison of the experimental leakage spectrum in air with the measured flux distribution in water. This comparison rests upon the assumption that the S_n calculation represents the spatial flux distribution correctly. While the S_n calculation can do this, the fineness and type of the angular quadrature set, the scattering order of the cross sections, the number of energy groups, and the method of averaging the cross section data are important when detailed agreement is sought. The 30-group P_3S_{16} calculation used in this report is based on the limited storage capability of the IBM-7094 computer. It was possible, for the bare source in water, to perform a P_3S_{32} calculation. This has the effect of raising calculated water fluxes at large distances from the source. Increasing the spatial mesh interval, beyond 10 centimeters, from 1 to 1.5 centimeters caused a lowering of the calculated fluxes at distances past 20 centimeters of more than 2 percent. Finer spatial mesh interval and greater S_n angular quadrature scattering order thus tend to increase the calculated flux at large distances for a given assumed source spectrum.

For comparison, removal of 1 percent of the total source neutrons from the group above 10 MeV will lower the calculated resonance flux beyond 70 centimeters about as

much as the difference between the solid line in figure 7 and the dashed line. It is believed that there is not a significantly larger fraction of neutrons in the first three groups than estimated in the solid line of figure 5.

The measured water distribution is not very sensitive, however, to changes in the source that merely shift small fractions to neighboring groups. The sensitivity of a change in the fraction below 1 MeV is of some interest, since this fraction was not independently determined. Removal of 2 percent of the total source from group 16, centered at 0.6 MeV, and increase of 2 percent in group 8 at about 5.2 MeV will adequately represent such a shift. The calculated distribution in figure 7 decreases by a maximum of 2.9 percent near a radius of 8 centimeters, is unchanged near 14 centimeters, and increases by as much as 3.6 percent from 30 to 40 centimeters. The uncertainty in the measured points is somewhat less in the respective ranges. The estimated virgin source fraction below 1 MeV, using the Perkins' evaluated (n, 2n) data is then 12.0±2.0 percent.

COMPARISON OF CALCULATED RESULTS USING TWO EVALUATED Be(n, 2n) DATA SETS WITH MEASUREMENTS IN WATER FOR SOURCE ENCLOSED WITHIN BERYLLIUM SPHERES

Measurement of the flux distribution in water at indium resonance energy for the Am-Be neutron source enclosed by a beryllium shell yields several quantities which can be calculated. The spatial neutron flux distribution and the number of neutrons slowing down are the most important. Spatial moments of the flux distribution can also be calculated. Two shells of beryllium were used in the experiments. The smaller shell was 1.91 centimeters thick and had an outside diameter of 10.16 centimeters. The larger shell was 7.0 centimeters thick and had an outside diameter of 20.32 centimeters.

Detailed Shapes of the Indium Resonance Energy Flux Distributions

Figures 9(a) and (b) show two experimental flux distributions in water along with their corresponding multigroup transport calculations. The S_n calculations in each case use an S_{16} angular quadrature order, P_3 elastic scattering order, P_0 (n, 2n) scattering order for Be, and 30 energy groups. Two S_n calculations were performed for each experiment. One of the calculations used Perkins' Be(n, 2n) evaluation to compute P_0 (n, 2n) down scattering transfer cross sections with the AGN-SIGMA computer program. The other calculation used Be(n, 2n) P_0 down scattering transfer cross sections

from the GAM-II computer program data files. Both calculations used the virgin source spectrum listed in table IV.

Differences between the calculations with Perkins' (n, 2n) data for Be and GAM-II Be(n, 2n) data are significantly large for the 7.0-centimeter-thick Be shell flux measurement shown in figure 9(a). The flux measurement for the 1.91-centimeter-thick Be shell shown in figure 9(b) indicates similar differences for the two calculations. In the 7.0-centimeter thick Be shell the calculation which used GAM-II Be(n, 2n) data does not fit the measurements. Only from about 10 to 15 centimeters is there agreement. From 15 centimeters on this calculated distribution is much larger in magnitude than the measured distribution. For this 7.0-centimeter-thick Be shell the calculation which used Perkins' Be(n, 2n) data does fit the measurements. From 15 to 30 centimeters this calculated distribution varies by only a few percent from the measured distribution. From 30 centimeters to the end of the measured data the calculated distribution is slightly lower than the measured distribution. The calculation is higher than the measurement from about 10 to 15 centimeters. Perkins' Be(n, 2n) evaluation includes alternative models for the multibody component. The calculations shown here as using Perkins' Be(n, 2n) data use the three-body phase space model for the multibody component. A calculation using Perkins' Be(n, 2n) data which uses the cluster model for the multibody component gives a generally poorer fit to the measured data for the 7.0-centimeter-thick Be shell experiment. The calculation with the cluster model component is lower than the calculation with the three-body component between 15 and 35 centimeters, the maximum difference being 6 percent at about 20 centimeters.

Remarks that were made previously concerning the detailed agreement of the transport calculation with the measurement for the bare source in water hold also for the calculations with the beryllium shell enclosed source in water. For example, to the extent that the calculated distribution is higher relative to the measurement in water at large distances from the source, the same should be true for the beryllium shell enclosed source in water results. In addition, the effect of neglecting the higher order Legendre components of the Be(n, 2n) down scattering transfer cross sections was estimated by calculating the indium resonance energy flux distribution using the 2.43-MeV excited state model for the total Be(n, 2n) cross section. Calculation of the flux distribution outside the 7.0-centimeter-thick Be shell, but near the shell, was about 2 percent lower when the P_1 down scattering transfer cross sections for the Be(n, 2n) reaction were included, which accounts for about 20 percent of the difference between the calculated and measured values in this region.

Although neutrons of a given energy slow down throughout the entire volume, the higher energy neutrons are more important at larger radii from the source. The calculation using the GAM-II Be(n, 2n) data shows more neutrons slowing down at radii greater than 15 centimeters than either the experiment or the calculation using the

TABLE VI. - PARAMETERS OF EXPERIMENTAL AND CALCULATED INDIUM RESONANCE ENERGY FLUX DISTRIBUTIONS FOR Am-Be SOURCE ENCLOSED BY Be SHELL FOLLOWED BY WATER

	1.9-cm-thick Be shell			7.0-cm-thick Be shell		
	Be(n, 2n) data	Experimental[a]	Calculated	Be(n, 2n) data	Experimental[a]	Calculated
Second moment, $\overline{r^2}\times10^{-2}$, cm^2	Perkins'	3.069 ([b]1.4)	3.074	Perkins'	2.419 ([b]1.4)	2.397
	GAM-II	3.092 ([b]1.4)	3.211	GAM-II	2.550 ([b]1.4)	2.696
Fourth moment, $\overline{r^4}\times10^{-5}$, cm^4	Perkins'	3.232 ([b]9.5)	3.391	Perkins'	2.003 ([b]10.6)	1.996
	GAM-II	3.257 ([b]9.5)	3.537	GAM-II	2.140 ([b]10.6)	2.322
Sixth moment, $\overline{r^6}\times10^{-8}$, cm^6	Perkins'	8.058 ([b]29.6)	9.273	Perkins'	4.625 ([b]33.4)	4.917
	GAM-II	8.121 ([b]29.6)	9.577	GAM-II	4.947 ([b]33.4)	5.582
Relaxation length, λ, cm	-------	8.96±0.10	-----	-------	9.00±0.10	-----

[a]Two experimental values for each moment correspond to use of calculated flux distribution in Be shell based on indicated Be(n, 2n) data set.

[b]Percent extrapolation for numerator (percent extrapolation for denominator ~0.1).

Perkins' Be(n, 2n) data. This emphasizes the fact that the Be(n, 2n) P_0 down scattering transfer matrix used by the GAM-II evaluation retains more high energy neutrons than does Perkins' evaluation.

The experimental moments for these cases are given in table VI. Moments obtained from the calculated distributions for the two Be(n, 2n) evaluations are also shown in table VI. As expected, agreement with experimental moments is better using the calculation with the Perkins' Be(n, 2n) data than with the GAM-II Be(n, 2n) data.

Calculated neutron flux energy spectra for the 7.0-centimeter-thick Be shell experiment are shown in figure 10. The calculation based on Perkins' Be(n, 2n) data is shown by the solid lines, while the calculation with GAM-II Be(n, 2n) data is shown by the dashed lines. The average energy is also given for each spectrum shown.

Enhancement Due to Beryllium

The volume integral of the indium resonance energy slowing down density is a measure of the number of neutrons slowing down past 1.45 eV per unit time per virgin source neutron. In addition to the production of neutrons by the (n, 2n) reaction in Be, there are high energy neutron absorptions in every isotope present except hydrogen. The net number of neutrons at 1.45 eV for the two Be shell experiments are related to a quantity called enhancement. The enhancement is defined here as the fractional increase in the

TABLE VII. - NEUTRON ENHANCEMENT FOR Am-Be SOURCE ENCLOSED BY Be SHELL FOLLOWED BY WATER

Experiment description	Be data set	Source augmentation[a]	Number of neutrons absorbed above 1.45 eV				Net number of neutrons slowing down past 1.45 eV	Relative enhancement, percent	
			Be in source	Source container and spacer if present	Be shell	Water		Calculated	Experimental[b]
Source in water	Perkins'	1.0486	0.0064	0.0007	------	0.0266	1.0149	----	--------
	GAM-II	1.0472	.0065	.0007	------	.0266	1.0134	----	--------
Source with 1.9-cm-thick Be shell	Perkins'	1.1572	0.0067	0.0011	0.0166	0.0220	1.1108 ([c]0.0089)	9.4	7.3±2.0
	GAM-II	1.1587	.0069	.0010	.0183	.0225	1.1100 ([c]0.0080)	9.5	7.2±2.0
Source with 7.0-cm-thick Be shell	Perkins'	1.3578	0.0068	0.0014	0.0540	0.0143	1.2813 ([c]0.0816)	26.3	23.5±2.5
	GAM-II	1.3817	.0071	.0012	.0651	.0150	1.2933 ([c]0.0675)	27.6	22.1±2.5

[a]Source augmentation is total virgin source neutron (1.0) plus number of neutrons produced by (n, 2n) reaction in Be.

[b]For 1.9-cm-thick Be shell experiment, estimated measured enhancement is taken to be 7.3±2.0 percent; for 7.0-cm-thick Be shell experiment, estimated measured enhancement is taken to be 22.8±2.5 percent.

[c]Net number of neutrons slowing down past 1.45 eV in Be shell.

number of neutrons slowing down past indium resonance energy for the source enclosed in a Be shell in water as compared to the source alone in water. Table VII shows the calculated neutron productions, absorptions, the net number of neutrons slowing down past 1.45 eV, and the enhancements. The fission and absorption cross sections of ^{241}Am are ignored in these calculations. The energy of 1.45 eV corresponds to the high energy boundary of group 28 listed in table II.

It should be noted that the indium resonance energy flux distribution was not measured in the Be shells. Therefore, to obtain the experimental enhancement, the calculated flux distributions were used for the Be shells. Although the contribution to the flux volume integral from the Be shells and source are large fractions of the total flux volume integral at indium resonance energy, their contribution to the slowing down integral is much less amounting to about 6 percent in the 7.0-centimeter Be shell experiment. The reason for this is that the ratio of the slowing down power of Be to that of water is 0.106. This value was based on the elastic scattering cross sections for Be and water. Equation (4b) is then used to calculate the total slowing down density at indium resonance energy.

If the enhancements in table VII are considered, not much significance can be attached to the fact that there is a slight difference between the two calculations of the enhancement in the experiment with the 1.9-centimeter-thick Be shell. In the experiment with the 7.0-centimeter-thick Be shell, however, the calculated enhancements differ: 26.3 percent using Perkins' Be(n, 2n) data and 27.6 percent using GAM-II Be data. When the experimental enhancements are considered, two values are shown because of the need to use calculated flux distributions in the Be shell. A reversal can be seen between the experimental enhancements and the calculated enhancements (i.e., 23.5 ± 2.5 and 22.1 ± 2.5 percent) for the experimental values using calculated Be shell flux distributions based on Perkins' and GAM-II Be(n, 2n) data, respectively. This results because there was, of course, only one experiment and the neutron flux distribution as calculated using Perkins' Be(n, 2n) data is higher than that using the corresponding GAM-II data.

The errors quoted on the experimental enhancements are the estimated standard error of the measurements and do not reflect the uncertainty in the flux in the Be shell and the source. Thus, in the 1.9-centimeter Be shell experiment the calculated value is just outside the 7.3 ± 2.0 percent estimated for the experimental value. In the 7.0-centimeter-thick Be shell experiment the enhancement calculated using Perkins' Be(n, 2n) data is just outside the error limit for the estimated experimental value. However, the calculated enhancement using GAM-II Be(n, 2n) data considerably exceeds the error limit for the experimental value. Thus, calculations using Perkins' Be(n, 2n) data are in better agreement with the experimental measurements than calculations using GAM-II Be(n, 2n) data. However, the results for these transmission experiments with Be shells

suggests the need for some revision of Perkins' evaluation for the (n, 2n) reaction in Be.

CONCLUSIONS

A number of conclusions concerning two Be(n, 2n) cross section evaluations result from this study of the measured indium resonance energy flux distributions in water due to neutrons transmitted through thick Be shells enclosing an americium-beryllium (Am-Be) source:

1. Multigroup P_3S_{16} transport calculations with a virgin source spectrum and Be(n, 2n) cross section data from Perkins' evaluation gave good agreement with indium resonance energy flux distribution measurements in water for the Am-Be source enclosed by Be shells.

2. Calculations with Be(n, 2n) cross section data from the GAM-II evaluation gave poor agreement with indium resonance energy flux distribution measurements in water for the Am-Be source within the Be shells.

3. For the Am-Be source in the 1.91-centimeter-thick Be shell, the computed enhancements are 9.4 and 9.5 percent for calculations using the evaluation due to Perkins for the Be(n, 2n) cross sections and the evaluation used by the GAM-II program, respectively. The experimental enhancement is 7.3±2.0 percent.

4. For the Am-Be source in the 7.0-centimeter-thick Be shell, the computed enhancements are 26.3 and 27.6 percent for calculations using the evaluation due to Perkins for the Be(n, 2n) cross sections and the evaluation used by the GAM-II program, respectively. The experimental enhancement is estimated to be 22.8±2.5 percent. The calculation using Perkins' evaluation for the Be(n, 2n) cross sections is better than that using the GAM-II evaluation.

5. These results show that the calculation of the spatial distribution of indium resonance energy neutrons and of the enhancement, as compared to the measurements, is significantly better using Perkins' evaluation for the (n, 2n) data for Be than the evaluation used by the GAM-II program. Since current ENDF/B cross sections are based on the same evaluation as used to formulate the GAM-II cross sections, it is suggested that the Perkins' evaluation be used to update cross sections for beryllium.

Lewis Research Center,
National Aeronautics and Space Administration,
Cleveland, Ohio, May 26, 1970,
129-02.

REFERENCES

1. Amster, H.; and Perkins, S. T.: A Calculation of the Age and Fast Effect in Beryllium and Beryllium Oxide. J. Nucl. Energy, vol. 21, no. 3, 1967, pp. 263-270.

2. Joanou, G. D.; and Dudek, J. S.: GAM-II. A B_3 Code for the Calculation of Fast Neutron Spectra and Associated Multigroup Constants. Rep. GA-4265, General Dynamics Corp., Sept. 16, 1963.

3. Joanou, G. D.; and Stevens, C. A.: Neutron Cross Sections for Beryllium. Rep. GA-5905, General Dynamics Corp. (NASA CR-54262), Nov. 13, 1964.

4. Anon.: ENDF Newsletter, vol. 4, no. 1, July 31, 1969. (National Neutron Cross Section Center, Brookhaven National Laboratory, Upton, N. Y.)

5. Perkins, S. T.: A Calculation of the Angular and Energy Distributions for Neutrons From the Be^9(n, 2n) Reaction. Rep. UCRL-50520, Lawrence Radiation Lab., California Univ., Oct. 4, 1968.

6. Perkins, Sterrett T.: The Be^9(n, 2n) Reaction and Its Influence on the Age and Fast Effect in Beryllium and Beryllium Oxide. Rep. AN-1443, Aerojet-General Nucleonics Corp. (AEC Rep. TID-22446), Oct. 1965.

7. Perkins, S. T.; Thompson, D. W.; and DuBois, P. J.: Users Manual for AGN-SIGMA: A Code to Calculate the Legendre Components of the Multigroup Transfer Matrices and the Group Cross Sections. Rep. AN-1447, Aerojet-General Nucleonics Corp. (AEC Rep. TID-22447), Oct. 1965.

8. Lombard, D. B.; and Blanchard, C. H.: Fission-to-Indium Age in Water. Nucl. Sci. Eng., vol. 7, no. 5, May 1960, pp. 448-453.

9. Wade, James W.: Neutron Age in Mixtures of D_2O and H_2O. Nucl. Sci. Eng., vol. 4, no. 1, July 1958, pp. 12-24.

10. Fieno, Daniel: Transport Study of the Real and Adjoint Flux for NASA Zero Power Reactor (ZPR-1). NASA TN D-3990, 1967.

11. Joanou, G. D.; Smith, C. V.; and Vieweg, H. A.: GATHER-II, An IBM-7090 Fortran-II Program for the Computation of Thermal-Neutron Spectra and Associated Multigroup Cross Sections. Rep. GA-4132, General Dynamics Corp., July 8, 1963.

12. Mynatt, F. R.; Greene, N. M.; and Engle, W. W., Jr.: On the Application of Discrete-Ordinates Transport Theory to Deep-Penetration Fast-Neutron-Dose Calculations in Water. Trans. Am. Nucl. Soc., vol. 9, no. 2, Nov. 1966, pp. 366-368.

13. Abramowitz, Milton; and Stegun, Irene A.; eds.: Handbook of Mathematical Functions with Formulas, Graphs, and Mathematical Tables. Appl. Math. Ser. 55, National Bureau of Standards, June 1964.

14. Hanson, A. O.: Radioactive Neutron Sources. Fast Neutron Physics. Vol. 1. J. B. Marion and J. L. Fowler, eds., Interscience Publishers, 1960, p. 3.

15. Bonner, T. W.; Kraus, Alfred A., Jr.; Marion, J. B.; and Schiffer, J. P.: Neutrons and Gamma Rays from the Alpha-Particle Bombardment of Be^{9}, B^{10}, B^{11}, C^{13}, and O^{18}. Phys. Rev., vol. 102, no. 5, June 1, 1956, pp. 1348-1354.

16. Gibbons, J. H.; and Macklin, R. L.: Total Neutron Yields from Light Elements under Proton and Alpha Bombardment. Phys. Rev., vol. 114, no. 2, Apr. 15, 1959, pp. 571-580.

17. Gibbons, J. H.; and Macklin, R. L.: Total Cross Section for $^{9}Be(\alpha, n)$. Phys. Rev., vol. 137, no. 6B, Mar. 22, 1965, pp. 1508-1509.

18. Risser, J. R.; Price, J. E.; and Class, C. M.: Resolved Neutrons from $Be(\alpha, n)$ Reaction. Phys. Rev., vol. 105, no. 4, Feb. 15, 1957, pp. 1288-1293.

19. Notarrigo, S.; Porto, F.; Rubbino, A.; and Sambataro, S.: Experimental and Calculated Energy Spectra of Am-Be and Pu-Be Neutron Sources. Nucl. Phys., vol. A125, 1969, pp. 28-32.

20. St. Romain, F. A.; Bonner, T. W.; Bramblett, R. L.; and Hanna, J.: Low-Energy Neutrons from the Reaction $Be^{9}(\alpha, n)C^{12}$. Phys. Rev., vol. 126, no. 5, June 1, 1962, pp. 1794-1797.

21. Gale, N. H.; and Garg, J. B.: The Population Ratio for the 4.433 MeV and 7.656 MeV States in ^{12}C in the Reaction $^{9}Be(\alpha, n)^{12}C$, and the Parameters of the 7.656 MeV Level. IL Nuovo Cimento, vol. 19, no. 4, Feb. 16, 1961, pp. 742-751.

22. Whitmore, B. G.; and Baker, W. B.: The Energy Spectrum of Neutrons from a Po-Be Source. Phys. Rev., vol. 78, no. 6, June 15, 1950, pp. 799-801.

23. Notarrigo, S.; Parisi, R.; Ricamo, R.; and Rubbino, A.: Neutrons from Po-Be Sources. Nucl. Phys., vol. 29, 1962, pp. 507-514.

24. Haag, D.; and Fuchs, H.: Die Energieverteilung der Neutronen aus einer Po-α-Be-Quelle. Zeit. f. Physik, vol. 174, June 4, 1963, pp. 227-230.

25. Broek, H. W.; and Anderson, C. E.: The Stilbene Scintillation Crystal as a Spectrometer for Continuous Fast-Neutron Spectra. Rev. Sci. Instr., vol. 31, no. 10, Oct. 1960, pp. 1063-1069.

26. Freestone, R. M., Jr.; Muckenthaler, F. J.; Straker, E. A.; and Henry, K. M.: Measurements of the Neutron Spectra of Po-Be, Pu-Be, and Am-Be Neutron Sources with an NE-213 Scintillator. Neutron Physics Division Annual Progress Report for Period Ending May 31, 1967. Rep. ORNL-4134, Oak Ridge National Lab., Aug. 1967, p. 25.

27. Verbinski, V. V.; et al.: The Response of Some Organic Scintillators to Fast Neutrons. Proceedings of the Special Session on Fast Neutron Spectroscopy presented at the 1964 Winter Meeting. Rep. ANS-SD-2, American Nuclear Society, Feb. 15, 1965.

28. Geiger, K. W.; and Hargrove, C. K.: Neutron Spectrum of an Am^{241}-Be(α, n) Source. Nucl. Phys., vol. 53, 1964, pp. 204-208.

29. Burrus, W. R.; and Verginski, V. V.: Recent Developments in the Proton-Recoil Scintillation Neutron Spectrometer. Proceedings of the Special Session on Fast Neutron Spectroscopy presented at the 1964 Winter Meeting. Rep. ANS-SD-2, American Nuclear Society, Feb. 15, 1965.

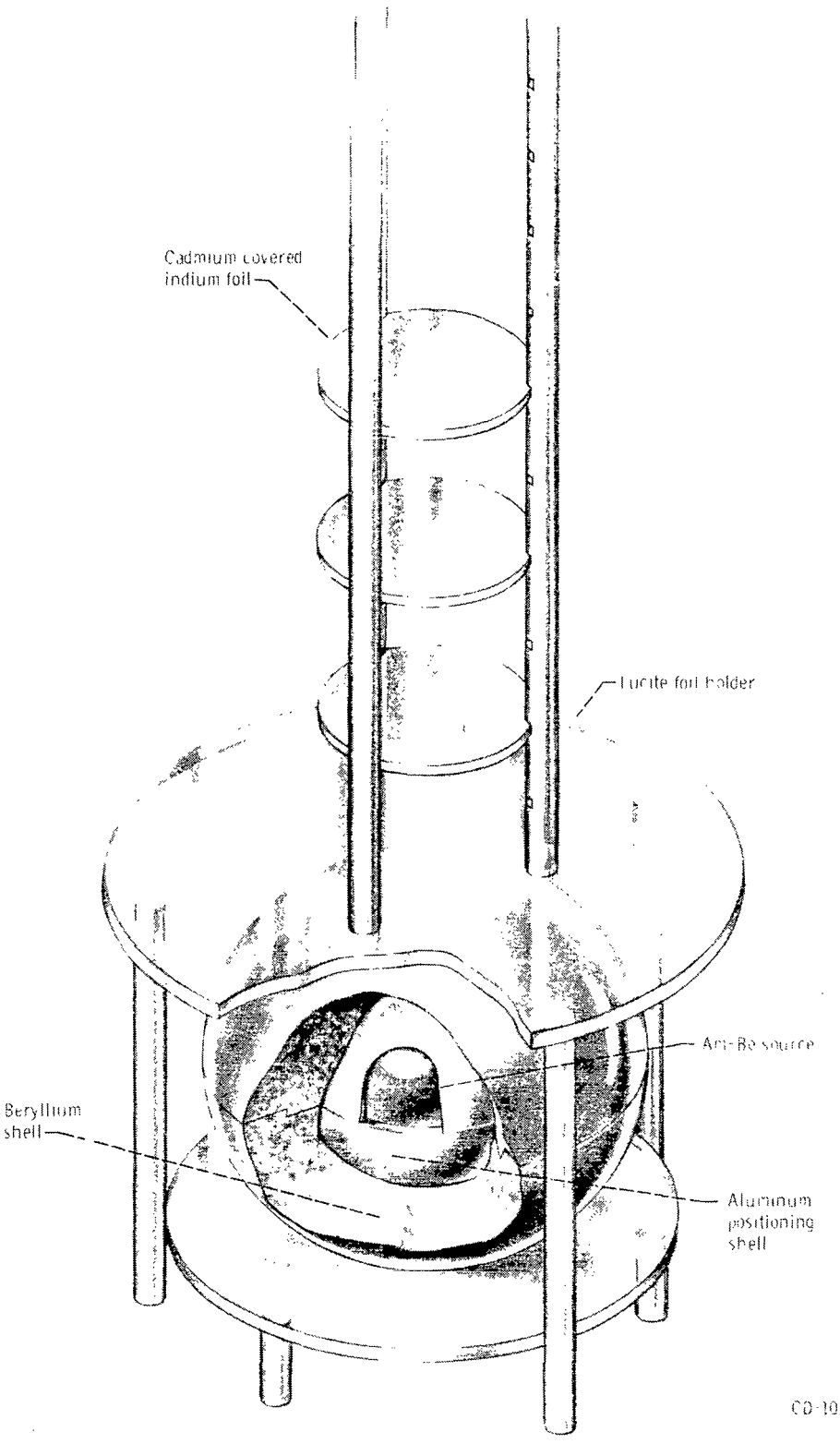

Figure 1. - Foil holder positioned over beryllium shell enclosing centrally located spherical americium-beryllium source.

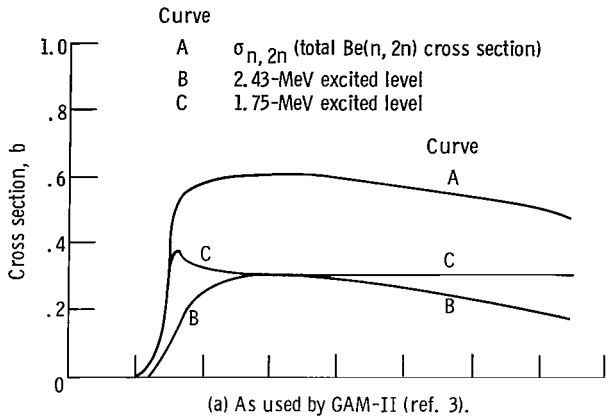

(a) As used by GAM-II (ref. 3).

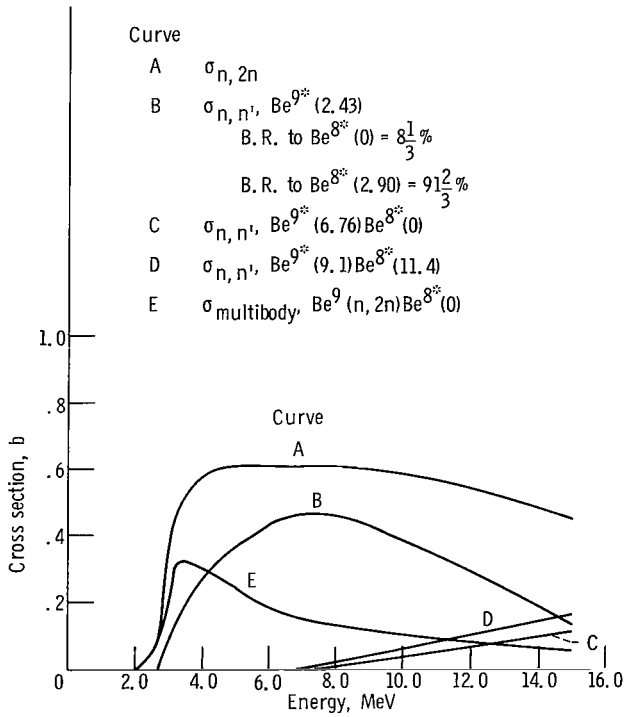

(b) Perkins' estimate (ref. 5).

Figure 2. - Cross sections for decay modes of Be(n, 2n) reaction.

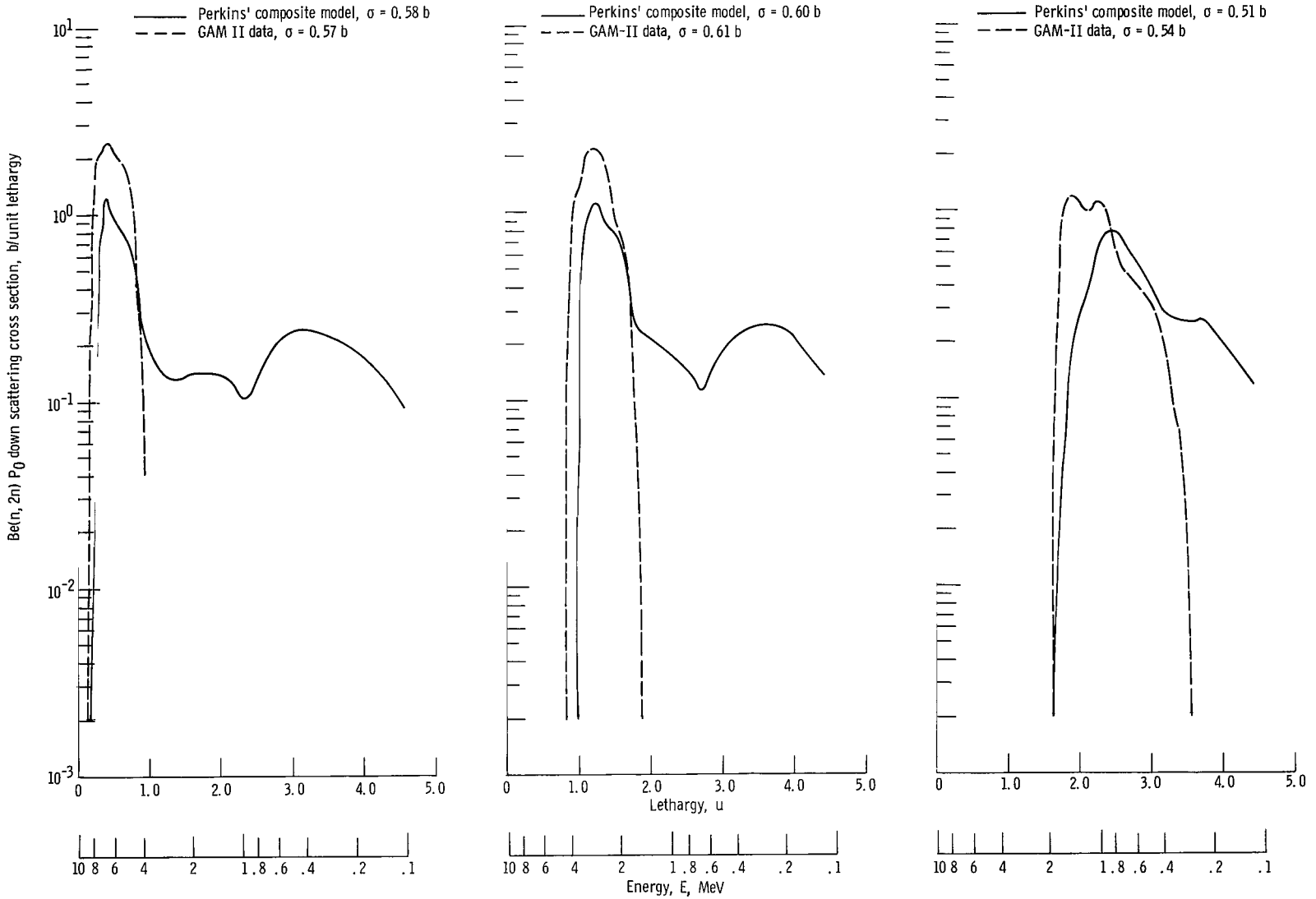

(a) For incident neutron energy of 9.5 MeV.

(b) For incident neutron energy of 5.8 MeV.

(c) For incident neutron energy of 3.5 MeV.

Figure 3. - Comparison of Be(n, 2n) P_0 down scattering cross sections for GAM-II and Perkins' evaluation.

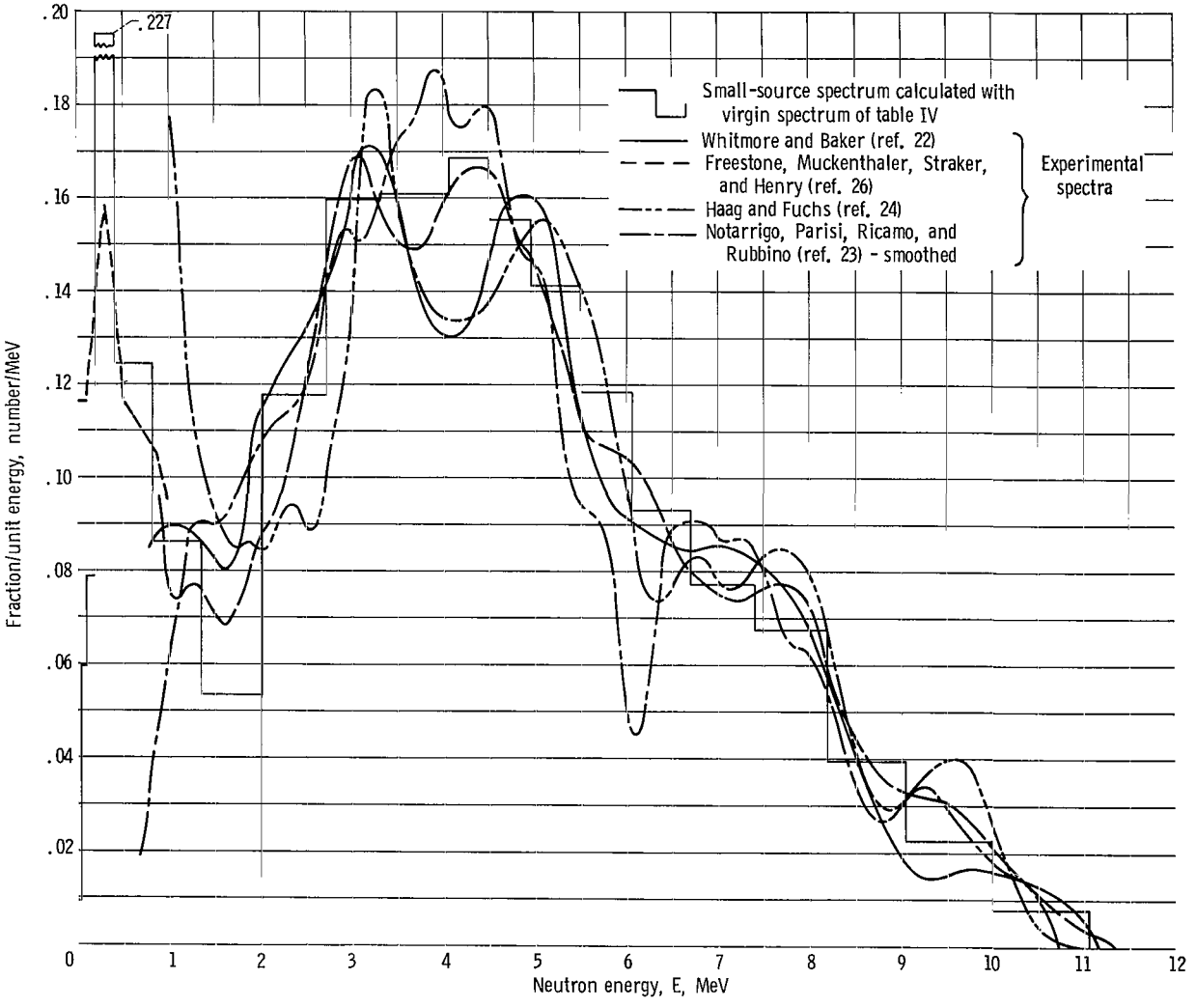

Figure 4. - Neutron spectra per unit energy for number of Po-Be sources.

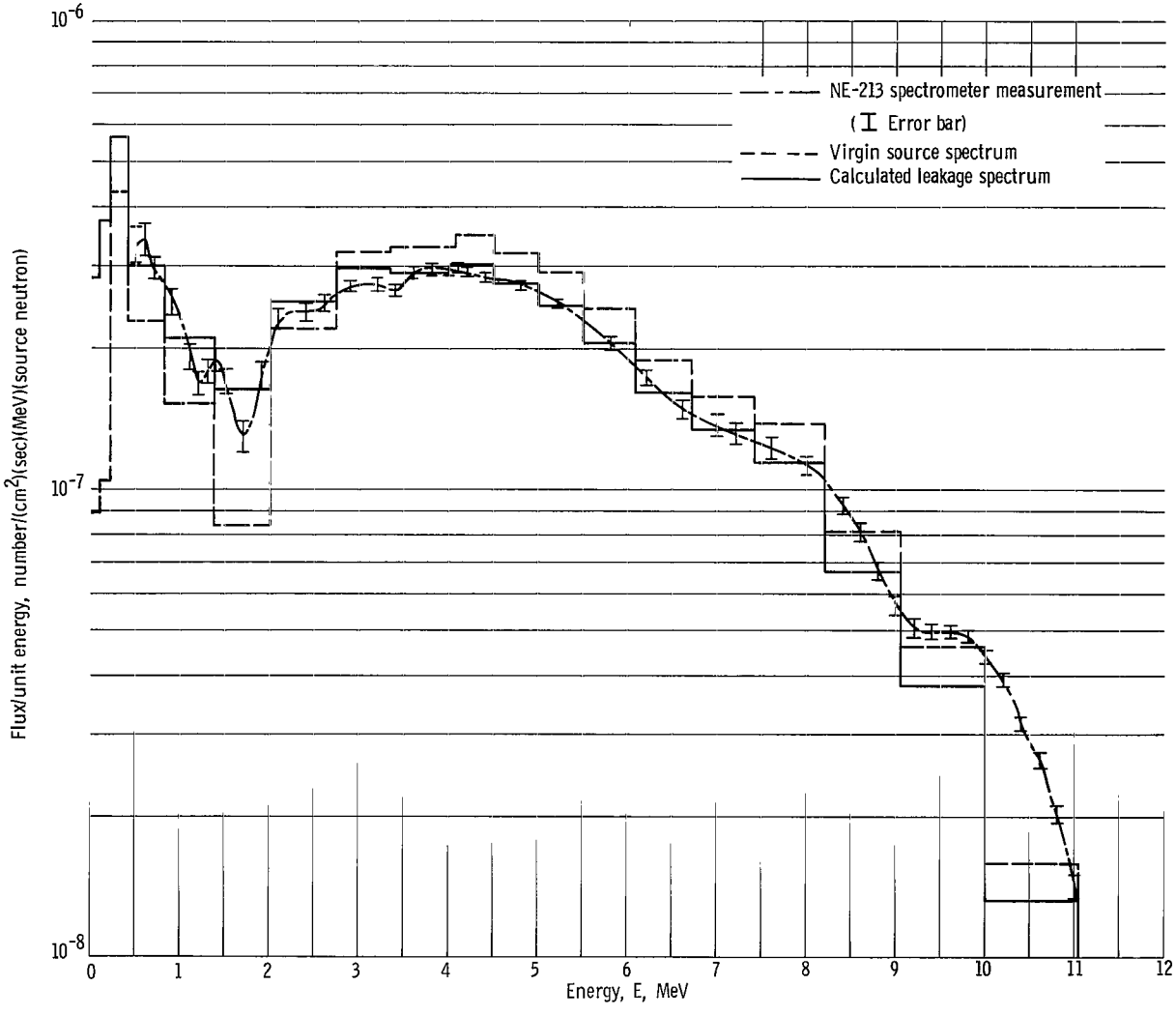

Figure 5. - Flux per unit energy at 2 meters for Am-Be source in air.

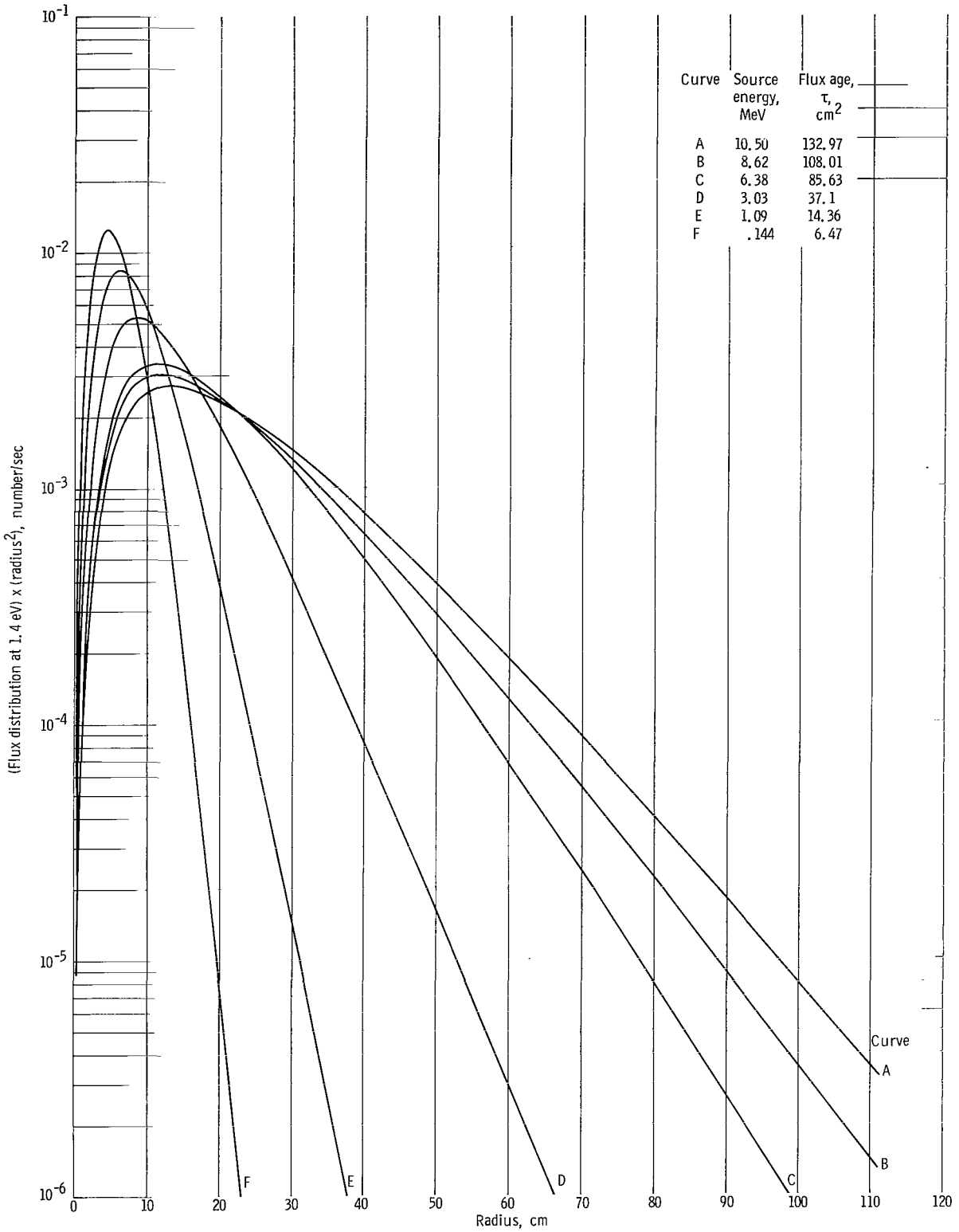

Figure 6. - Flux distribution times radius squared at 1.4 eV for point monoenergetic neutron sources in infinite water medium (P_3S_{16} multigroup transport calculation; normalization: volume integral = 1.0).

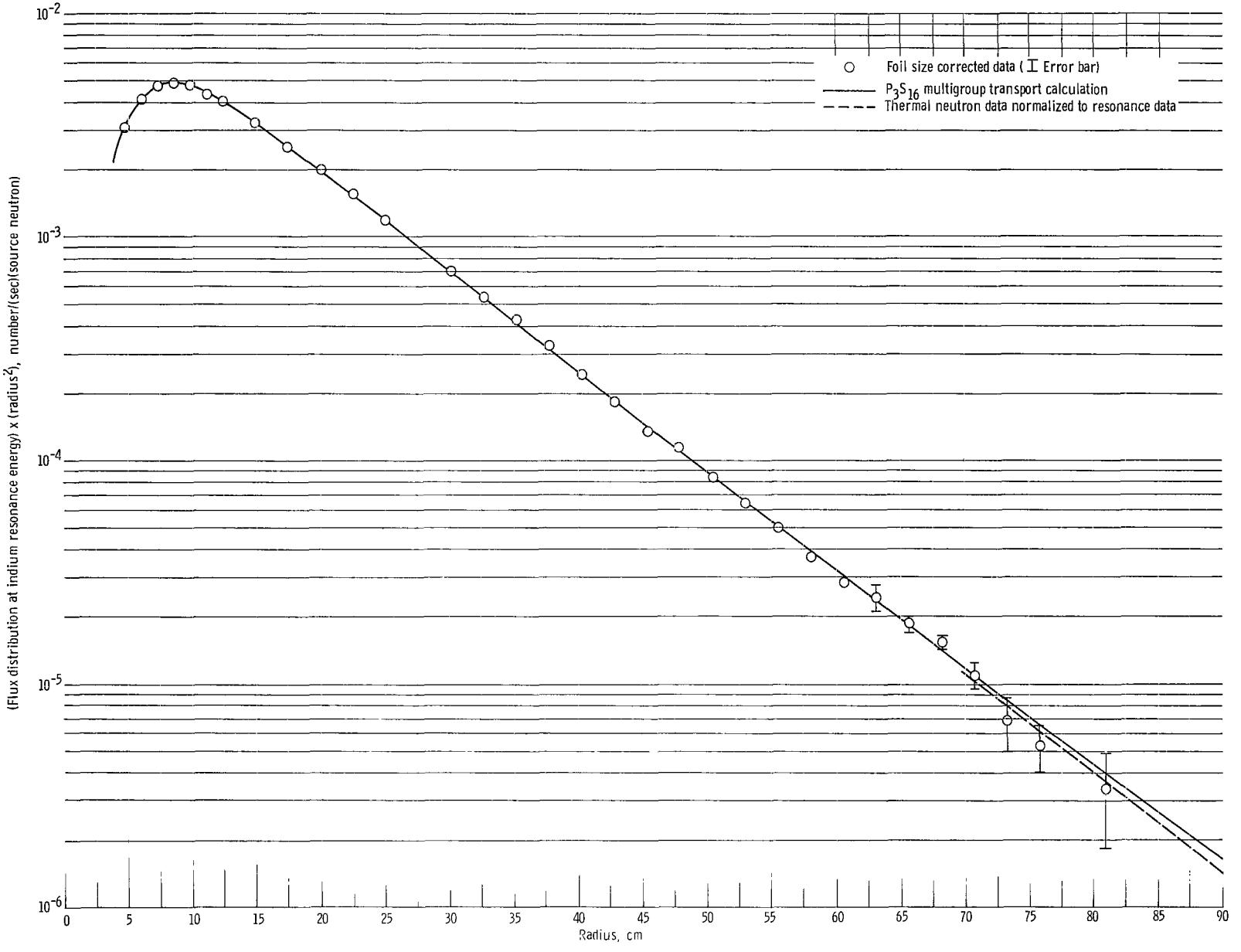

Figure 7. - Flux distribution at indium resonance energy times radius squared for Am-Be neutron source in water.

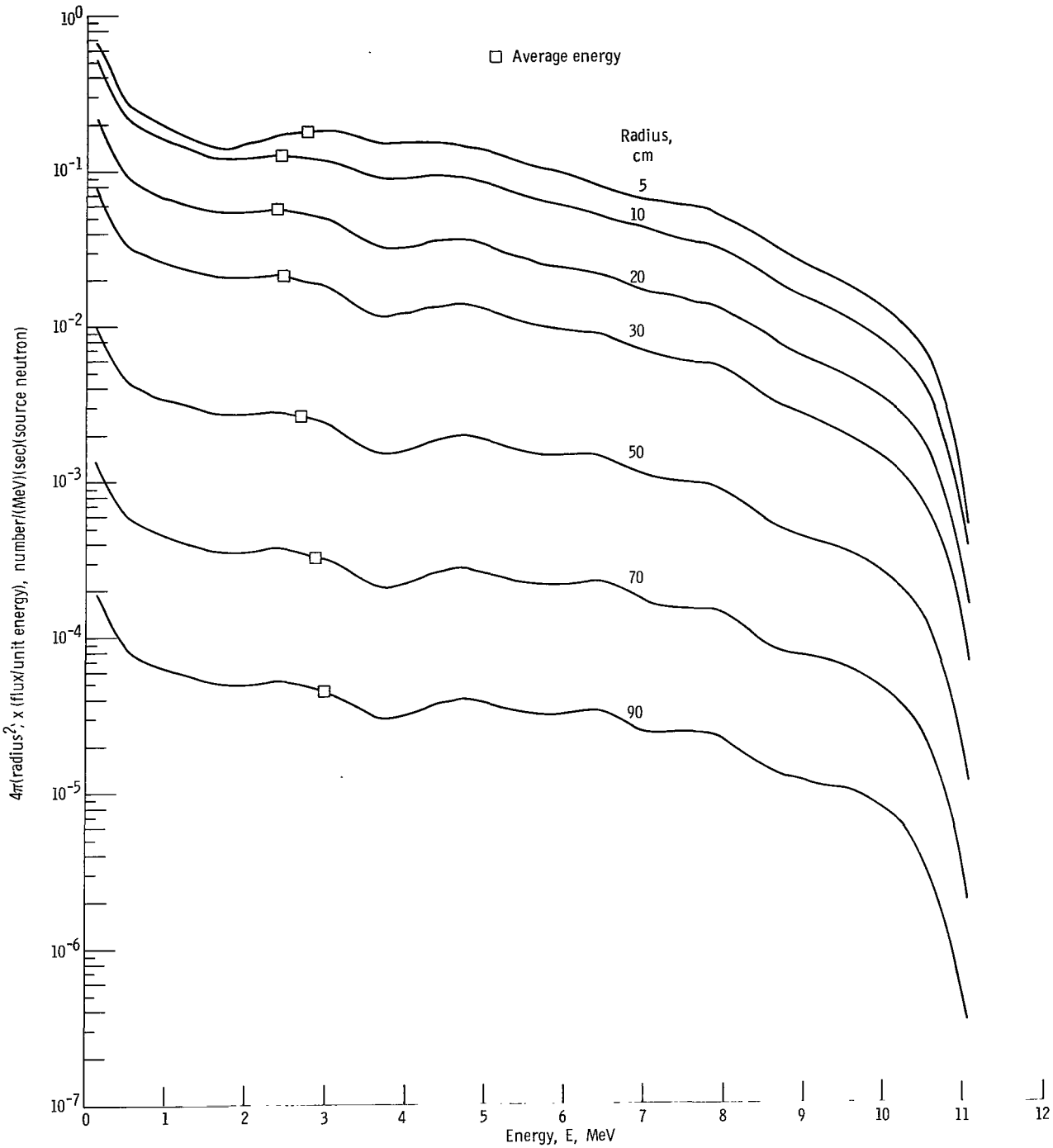

Figure 8. - Neutron spectra for Am-Be source in water medium.

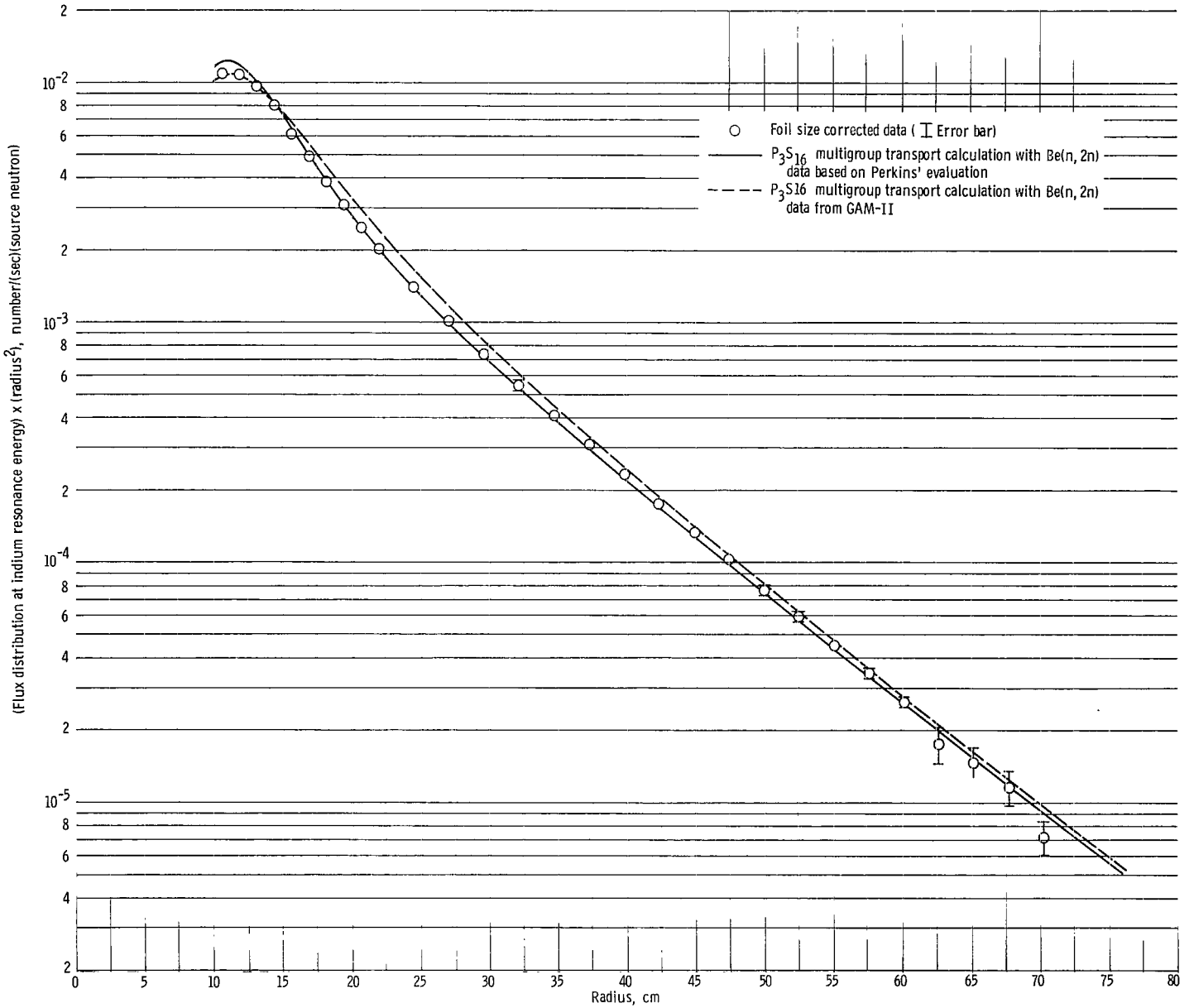

(a) Am-Be neutron source enclosed by 7.0-centimeter-thick Be shell followed by water.

Figure 9. - Flux distribution at indium resonance energy times radius squared.

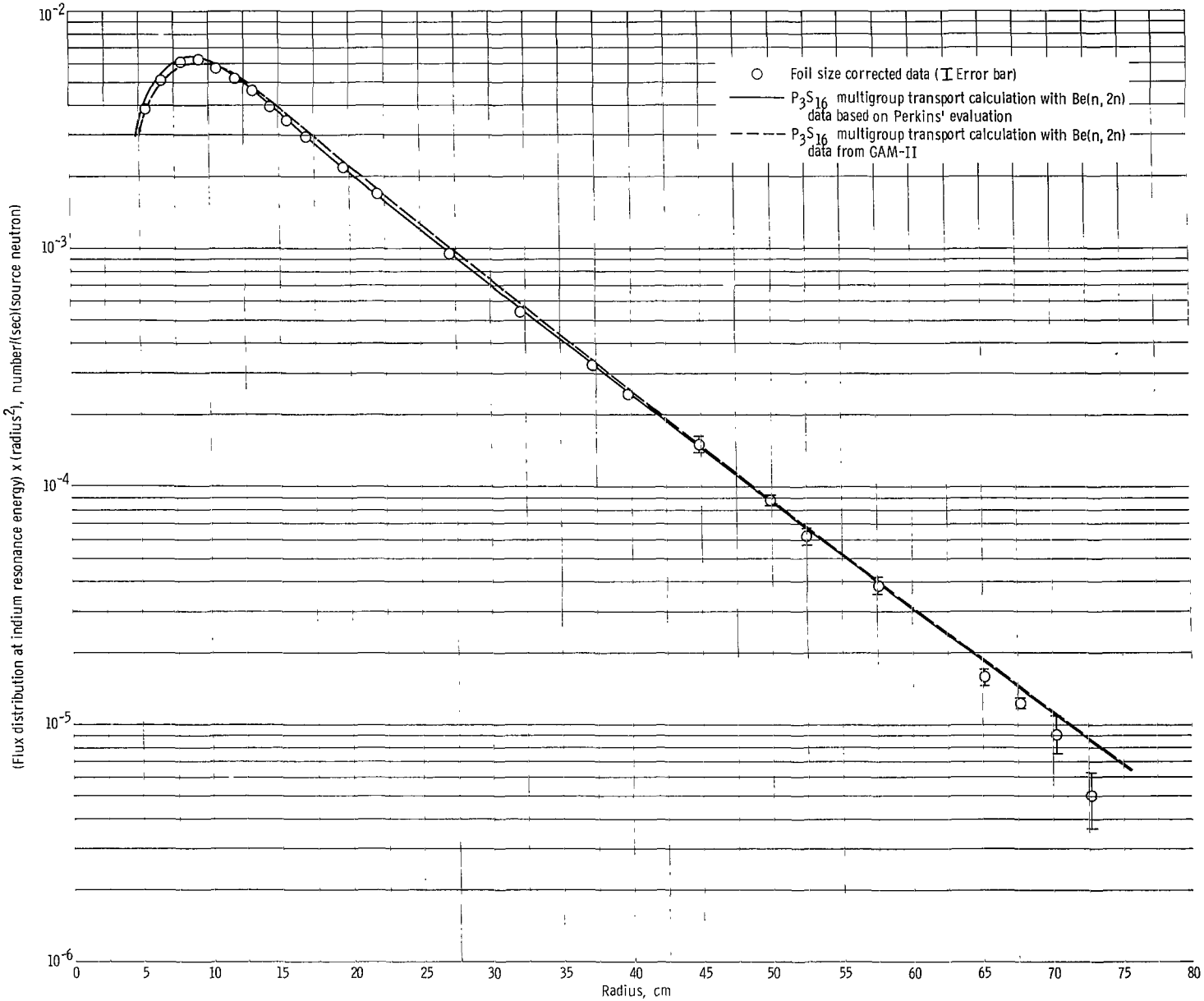

(b) Am-Be neutron source enclosed by 1.91-centimeter-thick Be shell followed by water.

Figure 9. - Concluded.

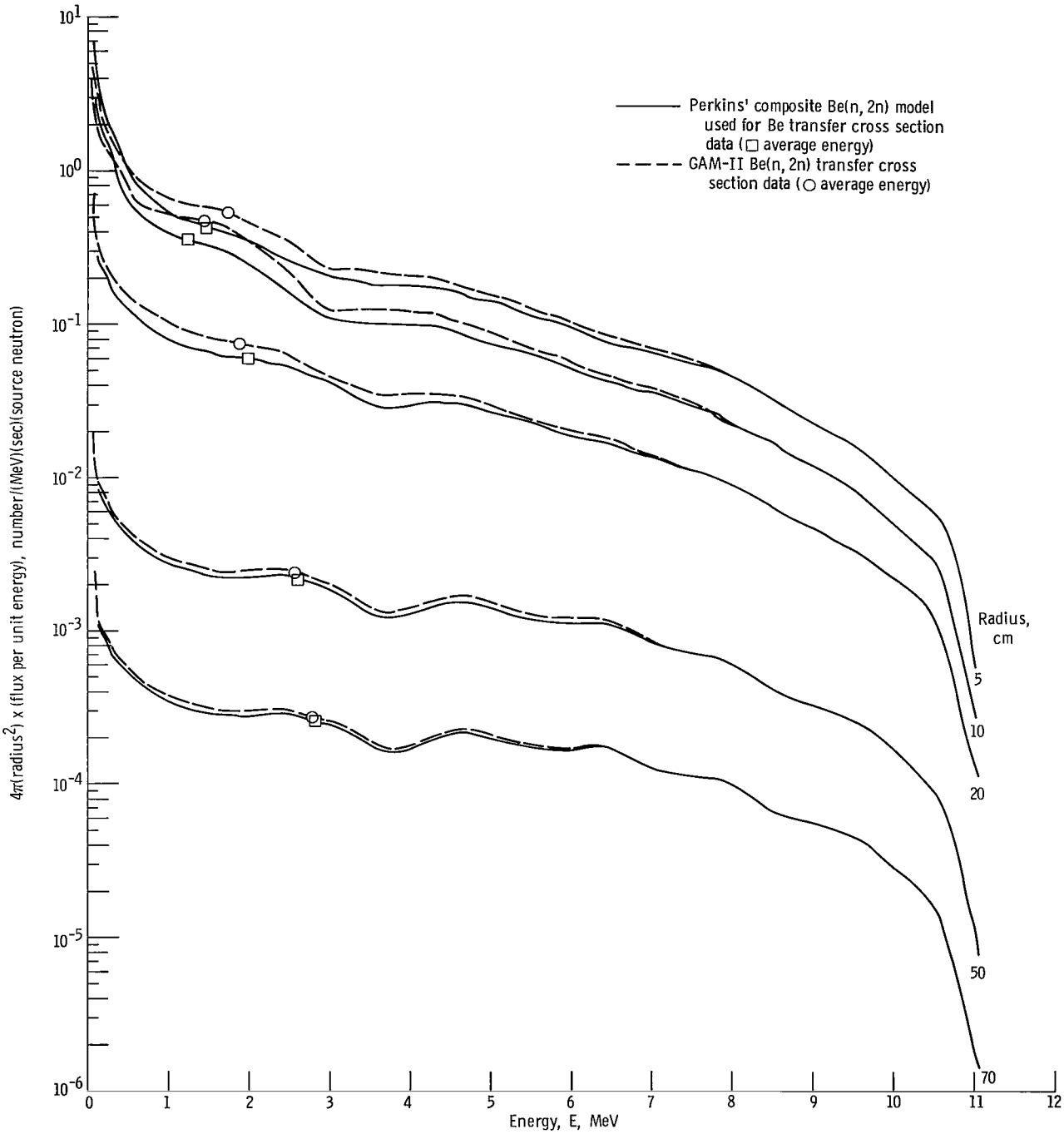

Figure 10. - Neutron spectra for Am-Be source enclosed in 7.0-centimeter-thick Be shell and followed by water.